NOVEMBER 30, 2017

PROJECT REPORT – GROUP 21

PARSHANT BOMBI | 301 255 126 | PBOMBHI@SFU.CA
GURDAS HOTHI | 301 291 936 | GHOTHI@SFU.CA
JONATHAN KIING | 301 276 654 | JKIING@SFU.CA
NAVJOT SINGH CHAHAL| 301 277 656 | NSCHAHAL@SFU.CA
SIMON FRASER UNIVERSITY

Table of Contents

Table of Figures

Abstract

While camping a person is far away from usual convenience and supplies that are readily available at home. This can lead to a myriad of problem that campers can potentially face, form insufficient heating to an absence of a light source a night, to even a deficiency of fresh water. These problems consistently plague campers regardless of where the actual camping location is. Therefore, given the opportunity to solve a problem faced the majority of campers, it is wise to choose the most serious problem faced by campers, a lack of fresh drinking water.

With this problem in mind, the team decided to set out to devise a way to solve it. Firstly, using A-type, T-type, and D-type elements, a rough design was constructed. The design consisted of both a storage section in which the energy was stored, and a dissipation section, in which the system performs the desired output by use of the stored energy. Following this, constitutive equations were used of develop the state space model of the system. Following his, model was further developed as the characteristics of the design parameters were sought after. Using the physical properties of materials, the values of the variables were determined.

Afterwards, the design parameters, in addition to the state space model, were then used and analyzed in MATLAB via ode45 in a linear, linearized and nonlinear fashion. These different types of analyzation techniques provided the required data needed to assess our initial design, and critique it.

Introduction

In modern society, rekindling with the wild and exploring the great outdoors is a large part of western culture. People typically experience the great outdoors by temporarily venturing into the nature by going on hikes, camping trips and expeditions. However, the great outdoors are vastly different from the safety and amenities society has provided, influencing outgoers to bring tools to aid their journey. With the aid of technology, explorers can travel deep into the great outdoors while remaining relatively safe and comfortable. Some of these technologies can provide warmth, sanitation and protection found out in the wild, providing the amenities humans desire that are not typically found in the wild unless built. And with these new technologies, campers can explore, enjoy and relax more than ever before.

Design Objectives

There are many beautiful camping sites around BC and one thing that almost all of them lack is a supply of pure drinking water. Thus it would be quite beneficial to help purify water. Therefore, because of this reason, the main objective we want to achieve with this design is to provide a safe, reliable and eco-friendly drinking water source. His object can only be accomplished by creating a device that can purify any kind of water available from the surrounding environment to safe drinking water by a natural means and at the same time avoiding any use of chemicals or hazardous devices. The device must be portable easy to setup and should be able to purify most of the impurities in water to make it safe for a human to ingest. Additionally, t should be wear resistant and be able to last for a long time.

Alternative Concepts

1- Heated Sleeping Bag

This concept is designed for colder conditions. The initial design uses a heated material within a sleeping bag to provide a heat source. It works using resistors which are then covered with a thick ceramic material. The heat generated by the resistors will be absorbed into the ceramic. The device will then be put inside of the sleeping bag, where it will slowly dissipate the heat stored into the insulated sleeping bag. The sleeping bag will be lined with these ceramic, providing many sources of heat throughout the sleeping bag, enabling for a more even distribution of heat. The device will be powered by either solar power or a gravity powered generator which can be plugged into the sleeping bag. This device speeds up the process of warming up the inside of the sleeping bag with your body heat or simply preheat the sleeping bag.
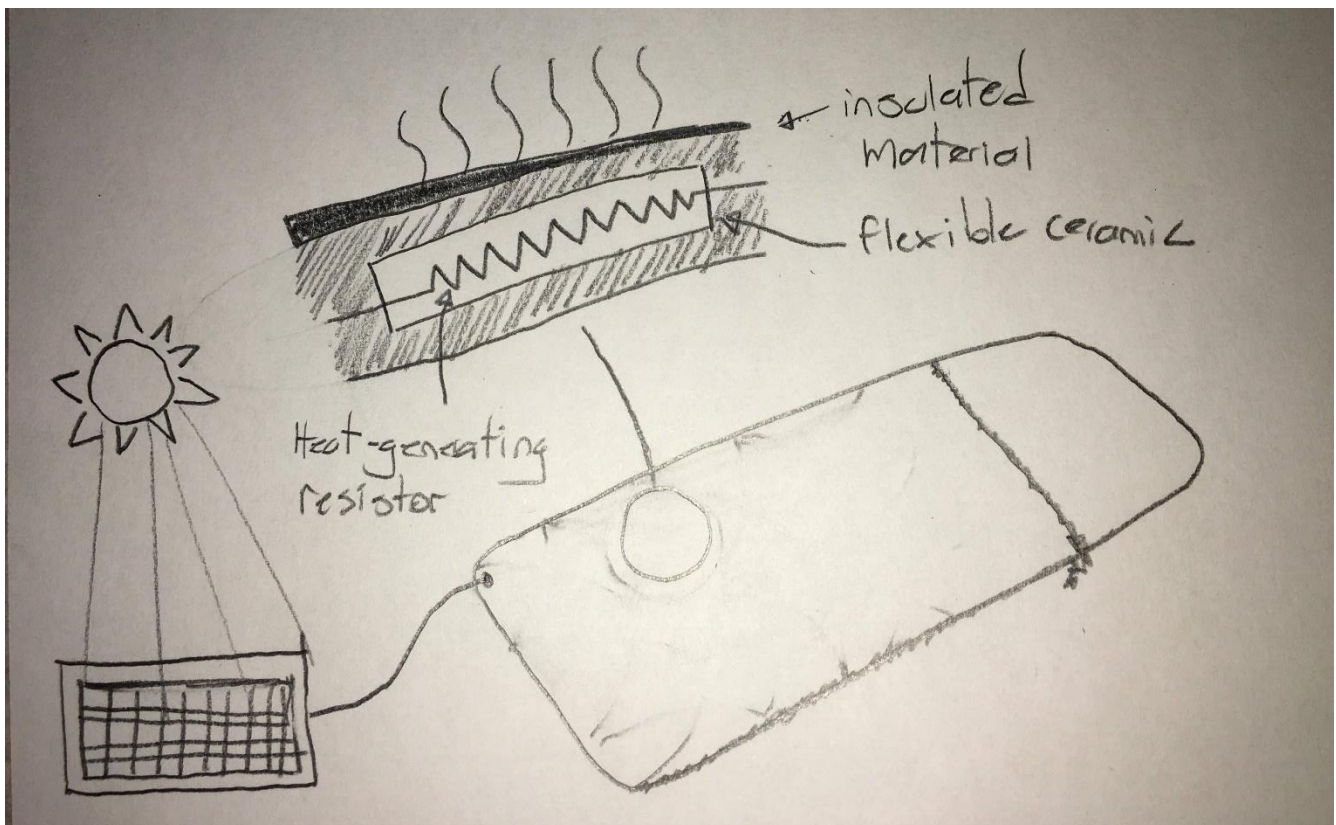
Figure 1: Heated Sleeping Bag Design Concept

2- Gravity Powered LED/Phone Charger

The first design that we came up with to solve this problem had a AC generator directly attached to a shaft. The generator had a hook at the top to hang it on any elevated object like a tree branch and then mass can be lifted to the desired height and then released to generate electricity. This system works by setting a heavy object up to a specified height and then releasing it, as the energy of this system is stored as gravitational potential energy. This causes the rope to unwind on a driving shaft thus creating a input torque to the system and then the angular speed of the shaft is increased with the pulley arrangement shown.
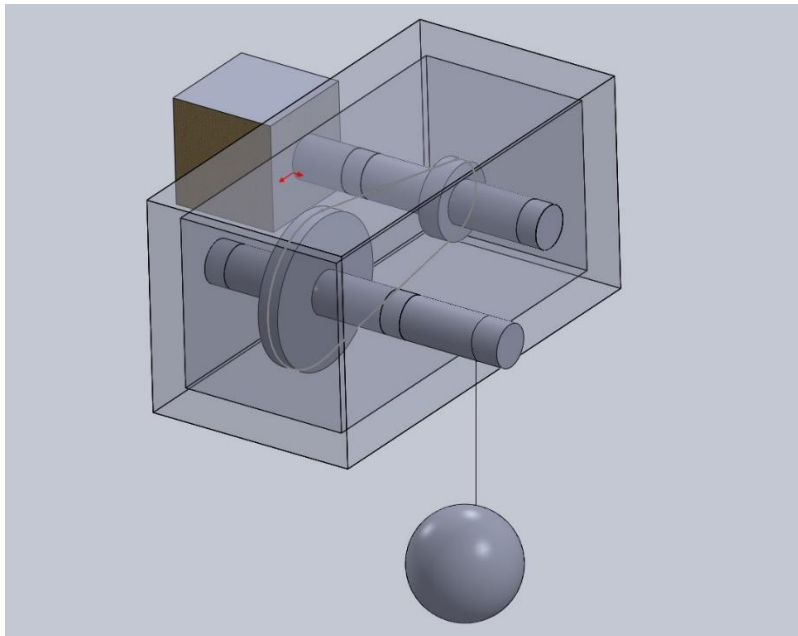
Figure 2: Gravity Powered LED/Phone Charger Design Concept

3- Gravity Powered Pump to Purifier

This design was inspired by the need to provide clean water in camping situations where clean water may not be easily accessible. Similar to the previous design, this concept uses of gravitational potential energy to store energy. By setting a mass up off the ground, and using the power of gravity as it falls down, one can convert this energy to power a pump which would force water through a filter and clean it.

Figure 3: Gravity Powered Pump to Purifier Design Concept

Design Selection

Since the main objective is to help with camping experience, we would like to have the most efficient and helpful device to aid the campers with. Therefore, when reviewing the previous designs, the following shortcoming were discovered:

1- Heated Sleep Bag

This concept's main problem was that it does not meet the minimum element count, it is less than 12 elements. Additionally this concept has other flaws which make it not ideal. Firstly, since this design may use solar panels, this would make it unreliable as throughout the day the amount of sunlight varies throughout the day, month, and year.

2- Gravity Powered LED Light

Main problem for this concept comes from the gravitational power source; recoiling the rope would be a bothersome task, as it requires someone to reset it. Additionally, if used in periods of darkness, resetting it could be dangerous, and therefore makes the whole function of the design counterproductive.

3- Gravity Powered Pump to Purifier

Likewise, for this design, recoiling the rope for the gravitational power source would be a nuisance. Another issue is fact of the extensive setup process required for initially the setup process as the mass needs to be hung at a height. But since is usable during all times of the day, a user could purify all the water they need when the sun is up, making it the most safe.

Final Selection Results

After considering these shortcomings, and weighing all our options, the group decided to go with the Gravity Powered Pump-to-Purifier design as it had the least amount of shortcomings in addition being the safest and most reliable design. The purely mechanical system and fluid based system with less elemental sensitive components entails that this device will be more dependable and can withstand the elements such as heavy rainfall or snow. Moreover, it provides a safe method to clean water without the use of heat or electricity, thereby making it environmentally friendly. This gravity powered pump is capable of filtering water in any location given the proper set-up, an incredibly useful advantage when living in the outdoors for extensive periods of time.

Design Description

There are a variety of portable devices and tools that are for the sole purpose of cleaning water. These include products such as water-soluble tablets, hand held filter pumps and even straws that filter water as the user can drink directly from the source. However, some of the problems with these products is that they are perishable (the water-soluble tablets) or providing larger amounts of clean water would take a long time (hand pumps). The goal of this design is to solve these problems, all while using a renewable energy source. The design can be hooked up to a tree or ledge where a nearby source of water can be filtered. A portable stand can also be used instead of a tree or ledge to provide the system with potential energy.

How it works

The device uses potential energy from a falling mass and converts it into kinetic energy of the water flow. It converts from one form of energy to the other by using a device connected to a pulley and a turbine. A mass is attached to a length of rope, where the rope is spooled around a pulley. The pulley is attached to a set of gears within the device which __+ or -__ the torque or angular velocity, driving the turbine to push water through a filtration device.

The first part of the design encompasses a mass connected to a rope, wound about a shaft. He mass takes gravity as the input of the system, and as the mass slowly drops downward, it rotates the shaft. This shaft is connected to a flywheel, which stores the energy as it is an A-type storage element. This flywheel is connected to another flywheel via a belt. This connection firstly helps increase the rotational speed of the second flywheel, however this belt also introduces slip, a nonlinearity.
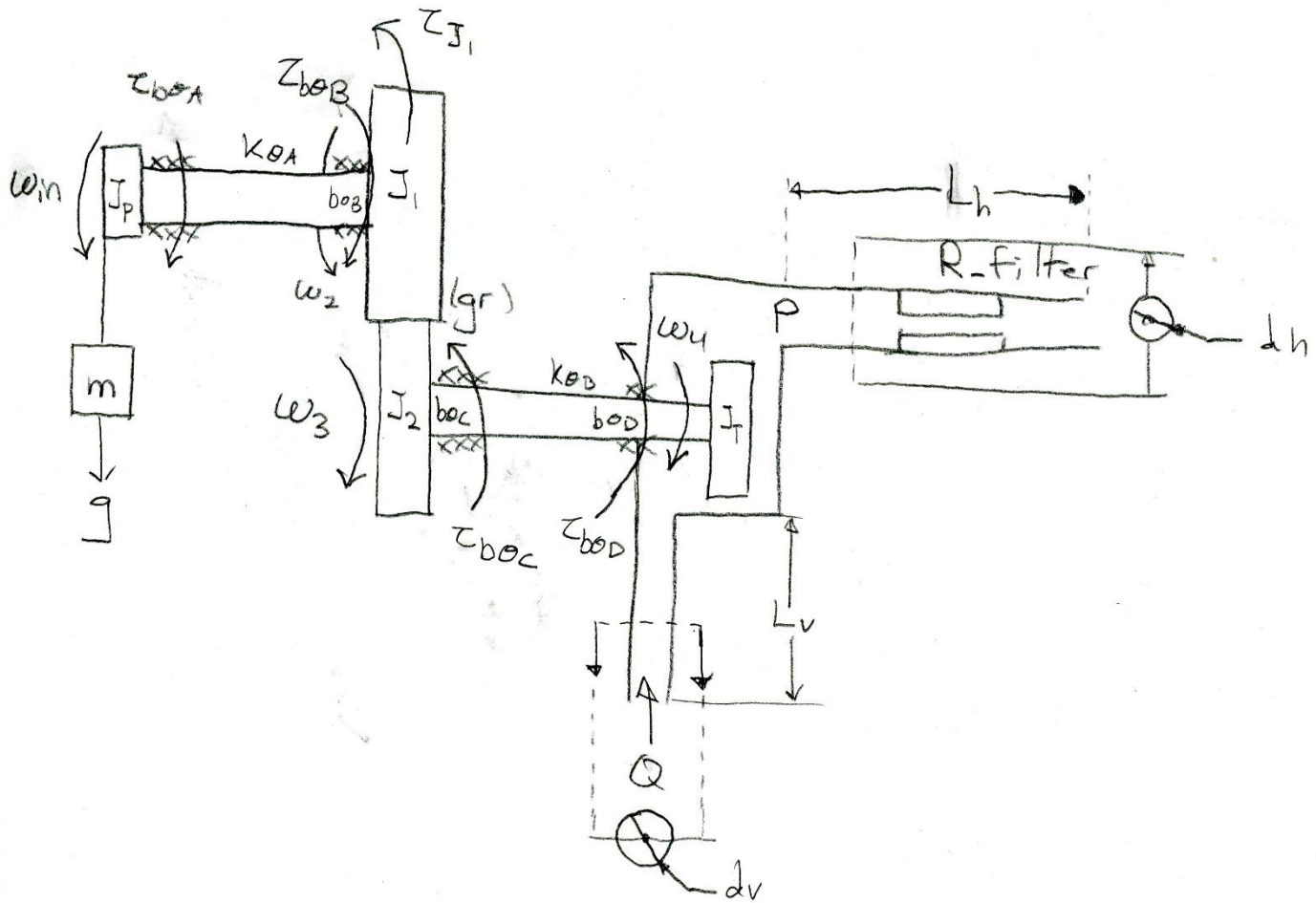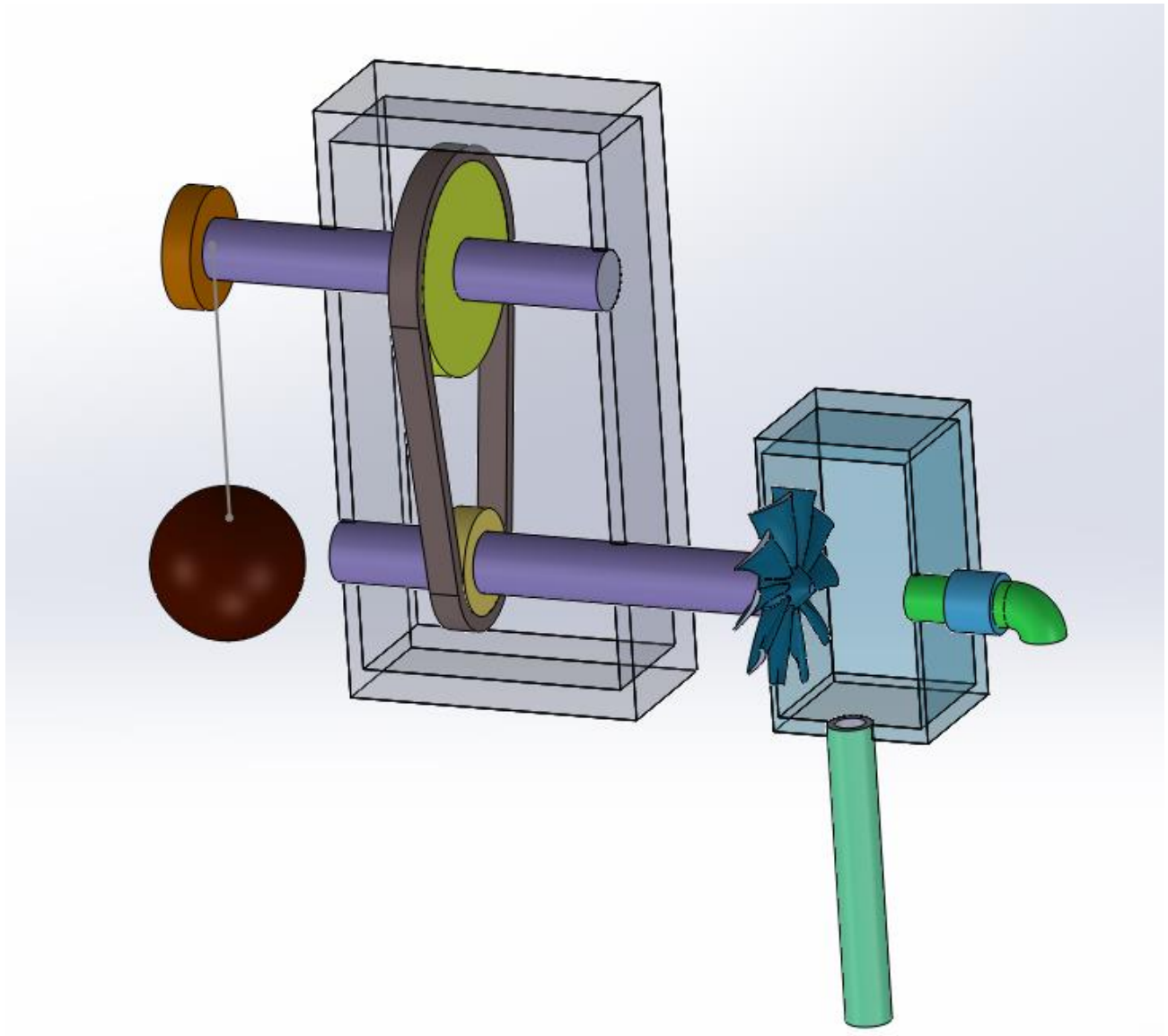
Figure 4: Sketch of model

Figure 5: Final Solidwork Assembly

How it is modelled

The system uses three different state model's scenarios, all are then linked together through constitutive equations to create a complete and cohesive simulation integrating all of the elements together.

Mechanical translational component

The first state model is fairly simple, as it is only a singular mass falling due to gravity. An upward for is applied from the rope the mass is attached to, which is translated into torque.

The second state model uses the potential energy of the falling mass and applies a force onto the rope, which then applies a force tangential to the radius of the shaft. The shaft is supported to resist lateral forces but not rotational forces, enabling it to convert the force of the mass's weight into a torque applied onto the shaft.

$$\tau = (F)\text{x}(r)$$

Mechanical rotational component

The force applied is transferred directly along the rope, where the rope unspools from the shaft in a tangential direction.

$$Torque\ applied\ to\ shaft = (weight\ of\ mass)\text{x}(radius\ of\ pulley) \rightarrow \tau_{mg} = (r_p)\text{x}(mg)$$

The inertia of the pulley and the torsional spring element attached to the mass acts as energy storage elements, while the friction acts as a resistance element. For the simulation, it was determined that the friction between shaft and housing was to be closer to the pulley, therefore the friction will be dependant on the angular velocity of the pulley.

$$\tau = J\alpha \quad \tau_{rotation} = b_\theta\omega \quad \tau_{rotational\ spring} = k_\theta\theta \quad \tau_{friction} = b_\theta\omega$$

Torque of friction: $\tau_{b_{\theta A}} = b_{\theta A}\omega_{in}$ Torque of spring A: $\tau_{k_{\theta A}} = k_{\theta A}\theta_{in} - k_{\theta A}\theta_2$

The Torque of the pulley can then be calculated using the sum of moments,

Sum of moments: $\sum \tau = J\alpha \quad J\alpha_{in} = \tau_{mg} - \tau_{b_{\theta A}} - \tau_{k_{\theta A}}$

$$\frac{d\omega_{in}}{dt} = -\frac{b_{\theta A}}{J_{Pulley}}\omega_{ing} - \frac{1}{J_{Pulley}}\tau_{k_{\theta A}} + \frac{r_p * m}{J_{pulley}}g$$

The torque of the shaft is then used to spin a gear, labelled J1. It is assumed that the relationship between J1 and J2 are a constant linear relationship: they have a fixed ratio. This also means that the angular velocity and acceleration are a scalar multiple of each other. It can also be assumed that the input of our system is gravity, which is a constant acceleration.

$$(gr) = gear\ ratio \quad \theta_3 = (gr)\theta_2 \quad \omega_3 = (gr)\omega_2 \quad \alpha_3 = (gr)\alpha_2 \quad T_{eq} = T_1 + T_2$$

Using the sum of moment equation again and the corresponding torques, 3 state equations were found:

$$\frac{d\tau_{k_{\theta A}}}{dt} = b_{\theta A}\omega_{in} - b_{\theta A}\omega_2 \qquad \frac{d\tau_{k_{\theta B}}}{dt} = k_{\theta B}(gr)\omega_2 - k_{\theta B}\omega_4$$

$$\frac{d\omega_2}{dt} = -\frac{b_{\theta B} + b_{\theta C} * (gr)}{J_1 + (gr)J_2}\omega_2 + \frac{1}{J_1 + (gr)J_2}\tau_{k_{\theta A}} - \frac{1}{J_1 + (gr)J_2}\tau_{k_{\theta B}}$$

The torque applied to the second rotational spring is then applied to the turbine. The friction between the shaft close to the turbine will be a function of the angular velocity of the turbine.

$$\tau_{JT} = \alpha_4 J_T = \tau_{k_{\theta B}} - \tau_{b_{\theta D}}$$

$$\tau_{b_{\theta D}} = b_{\theta D}\omega_4$$

$$\frac{d\omega_4}{dt} = \frac{1}{J_{turbine}}\tau_{k_{\theta B}} - \frac{b_{\theta D}}{J_{turbine}}\omega_4$$

The torque and angular velocity can then be used to calculate the flow rate and pressure by pump displacement equations. The pump is assumed to have a linear relationship with the torque and angular velocity of the turbine, where the relationships scalar multiples.

$$\tau = k_1 P \quad Q = k_2\omega$$

Fluid component

To fully model the hydraulic system, constituent subsystems are applied to the simulation, namely the fluid resistance and the fluid inertance. The equations used assumed constants for all resistances in the system, and its simplistic flow rate utilizing a single flow rate allows for the combination of all resistances into one value. The main sources of resistance in the fluid system is the vertical/horizontal length of pipe and the resistance of the filter. The resistance from the pipe can be calculated by:

$$R_v = 128\mu \frac{L_v}{\pi d_v^4} \text{ and } R_h = 128\mu \frac{L_h}{\pi d_h^4}$$

The resistance of the filter is found through empirical data given by the manufacturer of the product. An example graph is show below:
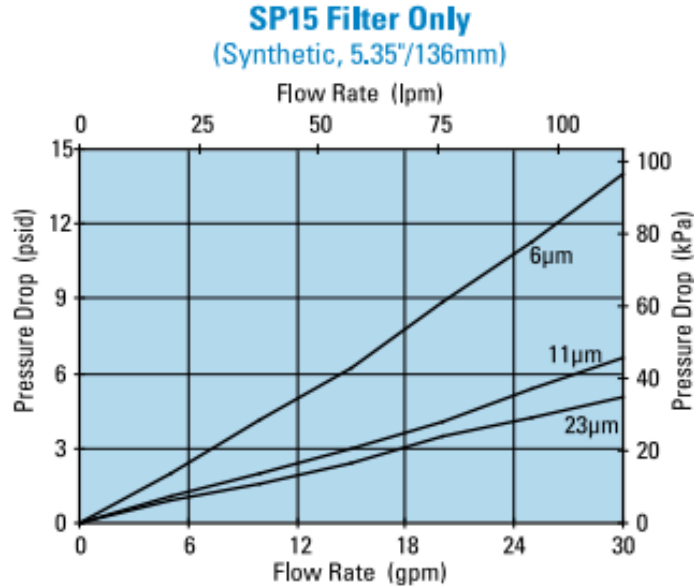

Figure 6: Filter resistance graph

The equivalent lumped resistance is given by summing the three resistances:

$$R_{eq} = R_v + R_h + R_f$$

The inertance of system can be calculated by:

$$I_v = \frac{8\rho}{\pi} \times \frac{L_v}{d_v^2} \text{ and } I_h = \frac{8\rho}{\pi} \times \frac{L_h}{d_h^2}$$

15

The equivalent lumped inertance is given by summing the two inertances

$$I_{eq} = I_v + I_h$$

Since there is only energy storing variable, there is only one state equation. The constitutive equations for the fluid resistor and inerter are:

$$\Delta P = R_{eq}Q \text{ and } \Delta P = I_{eq}\frac{dQ}{dt}$$

The pressure difference through out the system can as:

$$P_{1a} = P_{12} + P_{23}$$

Where:

$P_{1a} = P_s(t) = Pressure\ from\ pump$

$P_{12} = Pressure\ drop\ from\ lumped\ resistor$

$P_{23} = Pressure\ change\ from\ inertance$

Using the pressure differences and the constitutive equations we can create the state equation.

$$\frac{dQ}{dt} = \frac{1}{I_{eq}}\Delta P = \frac{1}{I_{eq}}P_{23} = \frac{1}{I_{eq}}(P_{1a} - P_{12}) = \frac{1}{I_{eq}}(P_s(t) - R_{eq}Q)$$

$$\frac{dQ}{dt} = -\frac{R_{eq}}{I_{eq}}Q + \frac{1}{I_{eq}}P_s(t)$$

The pressure created by the turbine has a linear relationship with the torue of the turbine, therefore it is possible to relate the output flow rate and the torque of the turbine.

$$P = k\tau_{turbine}$$

$$\frac{dQ}{dt} = \frac{K_1}{I_{eq}}\tau_{k_{\theta B}} - \frac{K_1\,b_{\theta D}}{I_{eq}}\omega_4 - \frac{R_{eq}}{I_{eq}}Q$$

Non-linear components

In the real world, the depicted model would not include any linear elements due to the amount of variables influencing the system, in which these variables are constantly changing and some act in a sporadic manner making their behaviour impossible to model. While some of these variations can have little to no effect on the output of the model, some non-linear components

have non-linear influences on the system, which are dependent on the certain elements and their current state and conditions. The chosen non-linear elements simulated are the slipping of the belt between the gear ratios and the filtration resistance.

The nonlinear relationship of the v-belt system is the efficiency of the v-belt is the relationship between the two sheaves and the belt. The current angular velocity of both sheaves and the speed of the v-belt contribute to the effective input and output speeds of the shives. The transfer of speed from the sheave to the belt is a function of its angular velocity and a certain efficiency ratio, assuming that the faster the sheave turns, the effective speed transferred from the belt to the sheave decreases at a linear rate. Due to two sheaves being used, the nonlinearity is the transfer of speed from the first sheave to the belt then the transfer of speed from the belt to the second sheave. This relationship can be modelled into an influence of the gear ratio between the two sheaves.

$$\eta = (gr)\left(1 - \frac{S}{100}\right) \quad (gr) = sheave\ ratio \quad \eta = speed\ transfer$$

$$S = s_1 + s_2$$

$$s_1 = A\omega_2 \qquad s_s = B\omega_3$$

Where ω_2 is the angular velocity of the first sheave and ω_2 is the angular velocity of the second sheave. However, in order to calculate η, ω_3 is needed. This is impossible to find due to needing the η to find the output angular velocity, the simulation used assumed that in order to calculated η, $s_s = B(gr)\omega_2$ so that the efficiency would then be a function of only the input speed aka ω_2.

$$\eta = (gr)\left(1 - \frac{(A+B*(gr))}{100}\omega_2\right)$$

The eta is implemented into the linear model by replacing the constant (gr).

The next non-linear element implemented is the fluid resistance of the filter. While no concrete equations could be found illustrating the non-linearity of the fluid system, there are graphs depicting the relationship between the pressure drop and the flow rate. The image from figure 4 was processed using an online website [put citation here of this website: https://apps.automeris.io/wpd/] where multiple plots were extracted. The data extrapolated was then put into Microsoft XL, where a function of the 2nd order was chosen to closely estimate the shape of the data. This allows for the simulation of the non-linear component as the relationship between pressure drop and flow rate provides a fluid resistance value.
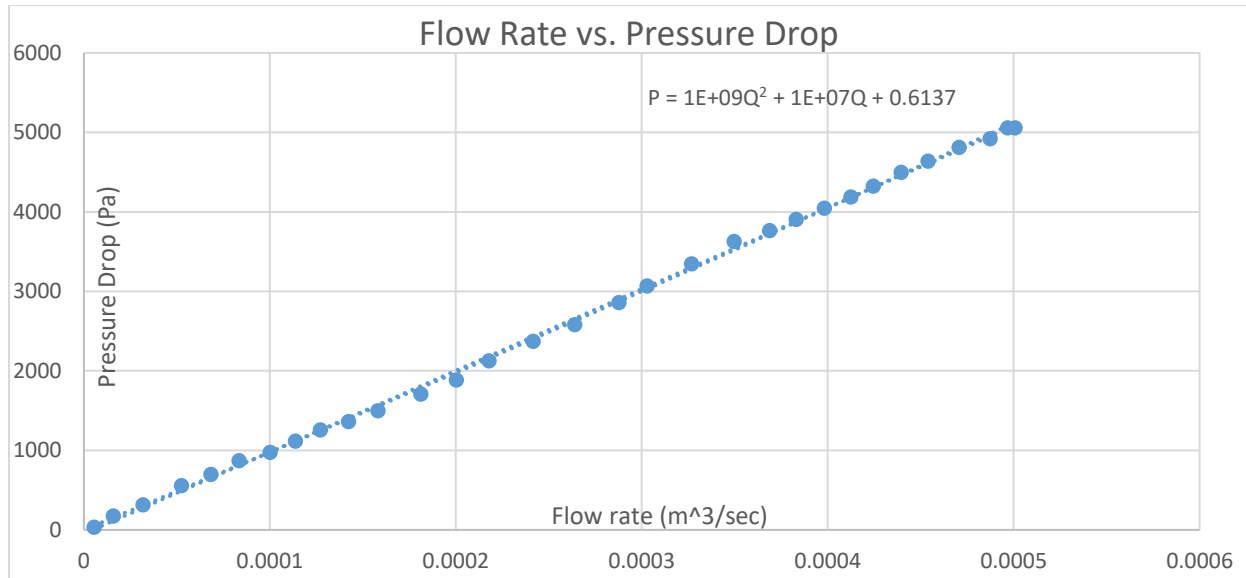
Figure 7: excel generated function of filter resistor

$$fluid\ Resistance = \frac{Pressure\ drop}{Flow\ rate}$$

$$fluid\ Resistance = \frac{(1\mathrm{x}10^9)Q^2 + (1\mathrm{x}10^7)Q + 0.6137}{Q}$$

$$fluid\ Resistance = (1\mathrm{x}10^9)Q + (1\mathrm{x}10^7) + 0.6137Q^{-1}$$

This value is then implemented into the equivalent fluid resistance equation, creating another non-linearity in the system.

Another possible non-linear element could be the influence of the dynamic viscosity (μ) of the water. This value directly influences the equivalent fluid resistance. While many variables effect this constant such as purity of water and the chemical composition of the lake water, a data table plotting the various values of μ dependant on temperature will be used for the effective μ value. However, the impact of temperature of was not included in the simulation, and instead only uses a constant for the dynamic viscosity.

18

System Modelling

Data Collection

After thorough research on potential camping sites, it was established that Chehal's river campground near Harrison Mills is one of better camping spots available. Such campgrounds are perfect for this or devised concept's application because there is a nearby water source, which need to be filtered before it is consumed.

After researching the environment of this campground, the average parameters of the campsite were found out. For instance, the average temperature there ranges from -1°C to-7 °C, during the winter, while in summer, the temperature range is from 10.7 to 18 °C. Diving deeper into the general environment for which this concept will be working in the following data was collected. The average wind speed in the region is in between 0-9 Km/h. Average humidity is greater than 70%. Average precipitation is around 1540 mm/year. A more precise average temperate able is shown below.

Months	Temperature		
	Normal	Warmest	Coldest
January	-2.0°C	0.7°C	-4.8°C
February	0.7°C	4.4°C	-3.0°C
March	4.5°C	9.9°C	-1.0°C
April	8.7°C	15.4°C	2.0°C
May	13.3°C	20.4°C	6.1°C
June	17.6°C	25.0°C	10.1°C
July	20.3°C	28.2°C	12.3°C
August	19.9°C	27.6°C	12.1°C
September	14.7°C	21.7°C	7.6°C
October	8.7°C	14.5°C	2.8°C
November	3.2°C	6.5°C	-0.3°C
December	-1.1°C	1.4°C	-3.7°C

Figure 8: Average Temperature of the southern BC Region

Element Modelling

1. Mass (m): The mass is modelled to be falling downwards only without considering any errors due to oscillations and other environment factors. Also the mass density is uniform and the mass is attached to the string from its center of gravity.
2. Inertia of rotating Pulley, Gear and Turbine pulley: While modelling, the inertia of the rotating pulley has been considered, but the model doesn't account for account for the unequal mass distribution in pulley that could cause it to wobble and dissipate some energy.
3. Friction at the pulley and gears: The model only consider constant friction coefficient and does not model any change in it due to increased rotation or change in temperature. Neither has it considered static friction which is greater than kinetic friction. It also doesn't considers the energy loss while the teeth of the gears hit together.
4. Rotating shaft: In reality excess torque can cause permanent strain in the connecting shafts which has been left out in modeling this machine.
5. Fluid inertance: The fluid is supposed to have a continuous streamline flow and model doesn't account for any irregular flow characteristics.
6. Filter Resistance: The resistance provided by the water filter that reduces the water flow is assumed to be uniform and doesn't considers any variations in its flow due to blocked portion or manufacturing errors.

Design parameters

SYMBOL	DEFINITION	REALISTIC VALUE
M	Mass of weight	10 kg
ρ	Density	8050kg/m^3
L_v	Length of Vertical Section of Pipe	0.5 m
L_h	Length of Horizontal Section of Pipe	0.2
d_v	Diameter of Vertical Section of Pipe	0.0254 m
d_h	Diameter of Horizontal Section of Pipe	0.0254 m
h	Thickness of Sheaves	0.01 m
K_{shaft}	Torsional Spring Coefficient	3836.84 Nm/rad
L_{shaft}	Length of Shafts	0.1 m
R_{shaft}	Radius of Shafts	0.0075
G	Modulus of Rigidity	77.2 GPa
J_{shaft}	Polar Moment of Inertia of Shaft	4.97×10^{-9}m^4
$J_{sheave1}$	Moment of Inertia of Larger Gear	7.899×10^{-4}kg m^2
$J_{sheave2}$	Moment of Inertia of Smaller Gear	4.940×10^{-5} kg m^2
J_{pulley}	Moment of Inertia of Pulley	7.903×10^{-3}kg m^2
μ	Dynamic viscosity	1.14 x 10^{-3} Pa*s
R_{filter}	Fluid Resistance	10500(N/m^2)/(m^3/s)
R_v	Resistance of Vertical Pipe	68521 (N/m^2)/(m^3/s)
R_h	Resistance of Horizontal Pipe	22318(N/m^2)/(m^3/s)
$J_{turbine}$	Moment of Inertia of Turbine	2.22×10^{-3} kg m^2
$M_{turbine}$	Mass of Turbine Impeller	0.907185 kg
$R_{turbine}$	Radius of Turbine Impeller	0.07 m
b_{thetaA}	Friction at Pulley	0.0015
b_{thetaB}	Friction of Sheave 1	0.0015
b_{thetaC}	Friction of Sheave 2	0.0015
b_{thetaD}	Friction of turbine	0.0015
k_1	Pump Displacement of CIPR	1.15

Torsional Spring Constant of Shafts

$$\theta = \frac{TL}{GJ}$$

$$T = K_{shaft}\theta \qquad J_{shaft} = \frac{\pi R_{shaft}^4}{2}$$

$$K_{shaft} = \frac{GJ_{shaft}}{L_{shaft}} = 3836.84 \ \frac{Nm}{rad}$$

The chosen material to fabricate the shafts of the design would be stainless steel due to its availability and material properties such as strength and its ability to resist rusting over long periods of time. Using an assumed shaft length for both shafts, the spring constant was found to be 191.85 Nm/rad [1].

Moment of Inertia of Sheaves and Pulley

The moment of inertia of the gears is dependent on the radius of the gears. The simulated design uses a large torque driving the first sheave, where the output of the turbine speed is very high. This implies a speed increase is transferred between the sheave ratio. A decided value of a 1:2 increase and therefore selected the first gear to have a radius of 5 cm and the second gear to have a radius of 2.5cm. The selection of stainless steel provides an average density of 8050 kg/m³.

$$J_{sheave} = \frac{MR^2}{2}$$

$$M_1 = \rho\pi R^2 h = (8050)\pi(0.05^2)(0.01) = 0.6319$$

$$M_2 = \rho\pi R^2 h = (8050)\pi(0.025^2)(0.01) = 0.1581$$

$$M_{pulley} = \rho\pi R^2 h = (8050)\pi(0.05^2)(0.1) = 6.322$$

$$J_{sheave1} = \frac{M_1(0.05)^2}{2} = 7.899 \times 10^{-4} \qquad J_{sheave2} = \frac{M_2(0.025)^2}{2} = 4.940 \times 10^{-5}$$

$$J_{pulley} = \frac{M_{pulley}(0.05^2)}{2} = 7.903 \times 10^{-3}$$

Displacement of Pump

The displacement of the pump is usually a nonlinear term given by the following formula below but for ease of calculation we assumed a static flow rate and pump rpm of 3 liters/s and 1000 rev/s respectively.

$$Pump\ Displacement = \frac{231 \times GPM}{RPM} = \frac{231 \times 15.85 \times 3}{\frac{60}{2\pi} \times 1000} = 1.15$$

Resistance of Filter

Was found using a manufacture's performance data for a 23 micron filter. Since the flowrate of the entire system is relatively low an assumption had to be made from figure 4. The filter resistance can be found using the constitutive equation for a fluid resistor. Using the conversion factors lpm=0.000017 m³/s and kpa=1000Pa and using an average flow rate and pressure drop, a constant of about 10500 $\frac{N/m^2}{m^3/s}$ is used.

Dynamic viscosity

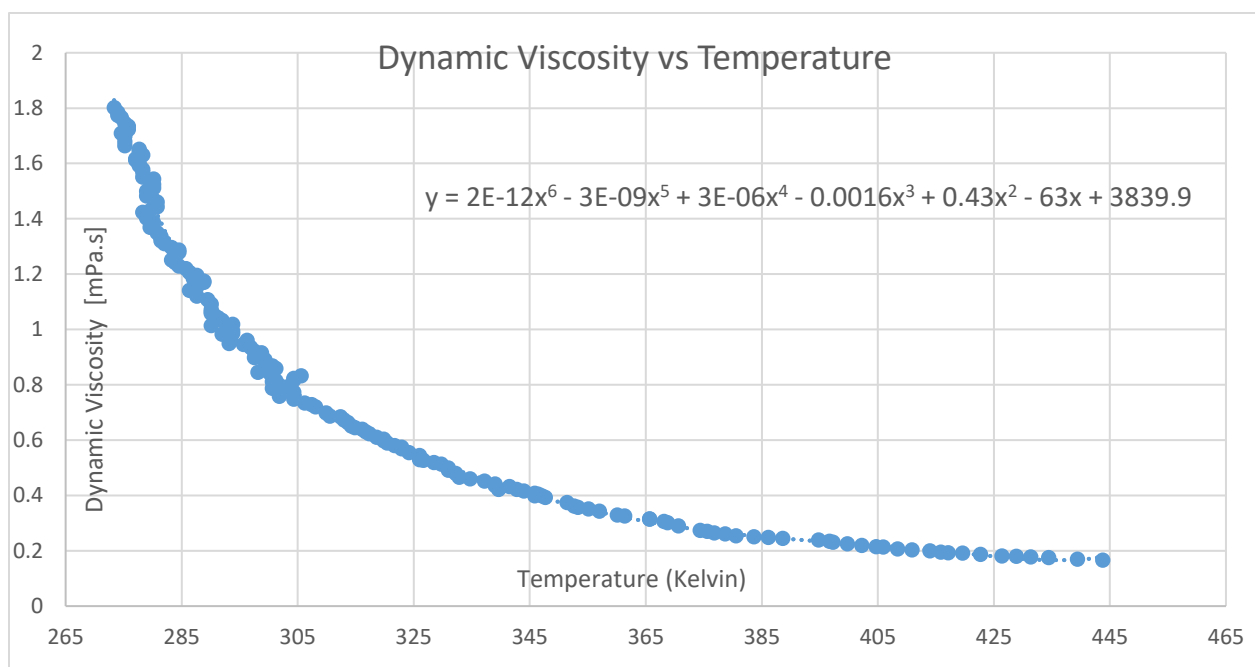The μ known as the dynamic viscosity of the fluid, is a specific value given by the current state of the fluid.

Figure 9 Dynamic viscosity

An average temperature of 10°C was used for an average μ value. A value of 1.14mPa*s was found or 1.14 x 10⁻³ Pa*s.

Resistance of Pipes

The pipe resistance from the horizontal and vertical sections can be modeled using the following equations:

$$R_v = 128\mu \frac{L_v}{\pi d_v^4} \qquad\qquad R_h = 128\mu \frac{L_h}{\pi d_h^4}$$

$$R_v = 68521 \frac{N/m^2}{m^3/s} \qquad\qquad R_h = 22318 \frac{N/m^2}{m^3/s}$$

Inertance of Pipes

The inertance of the pipes can be found using the following equations:

$$I_v = \frac{8\rho}{\pi} \times \frac{L_v}{d_v^2} \qquad\qquad I_h = \frac{8\rho}{\pi} \times \frac{L_h}{d_h^2}$$

$$I_v = 1973525.241 \qquad\qquad I_h = 789410.0966$$

Moment of Inertia of Turbine

The turbine moment of inertia was found by assuming that it was flat solid disc. All the data is directly from the manufacturer's website [2]. The inertial constant, k, for the moment is determined empirically [3].

$$J_{turbine} = kM_{turbine}R_{turbine}^2$$

$$J_{turbine} = 0.5 * 0.907 * 0.07^2 = 2.22 \times 10^{-3}$$

Mechanical Friction

The shafts are to be held in place by deep groove ball bearings therefore the rotational friction of the pulley, sheave 1, sheave 2 is 0.0015 [4].

Outputs and results

Linear Storage

The system was designed such that as the mass is lifted, it gains potential energy, this energy is then later used for the purification process. When modelling the energy storage phase of the concept, we firstly assumed that a constant force of 99 N was being applied, to lift up the mass, which has a weight of 98.1 N. This force profile was assumed to be constantly acting upon the rope at every second. The assumed force profile is shown below:
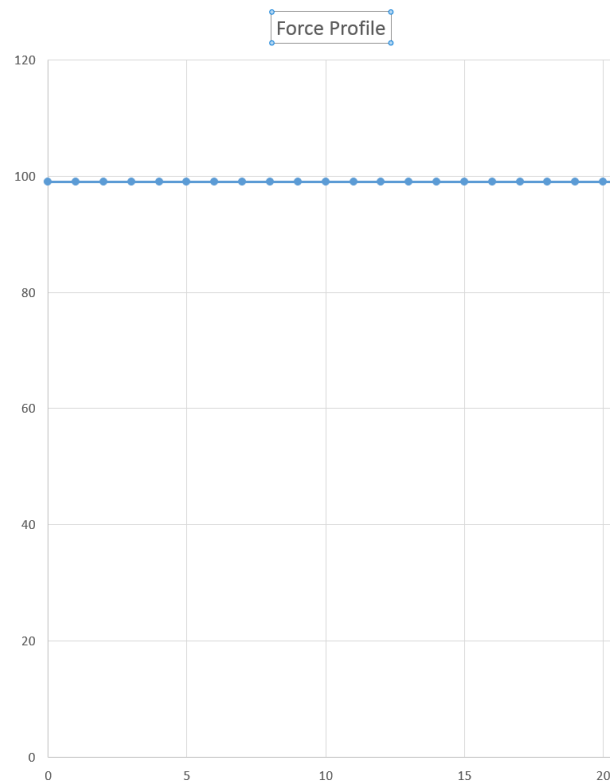
Figure 10: Assumed Force Profile

Using this force profile, it was found that the velocity of the mass being raised up was

$$v = (F_{in} - m * g)/m$$

Using this equation in addition to MATLAB's ode45, it was found velocity profile of the mass was found. This data was then used to determine the height of the mass at any given time, and the potential energy of the mass as well. These values are shown in the plots below.
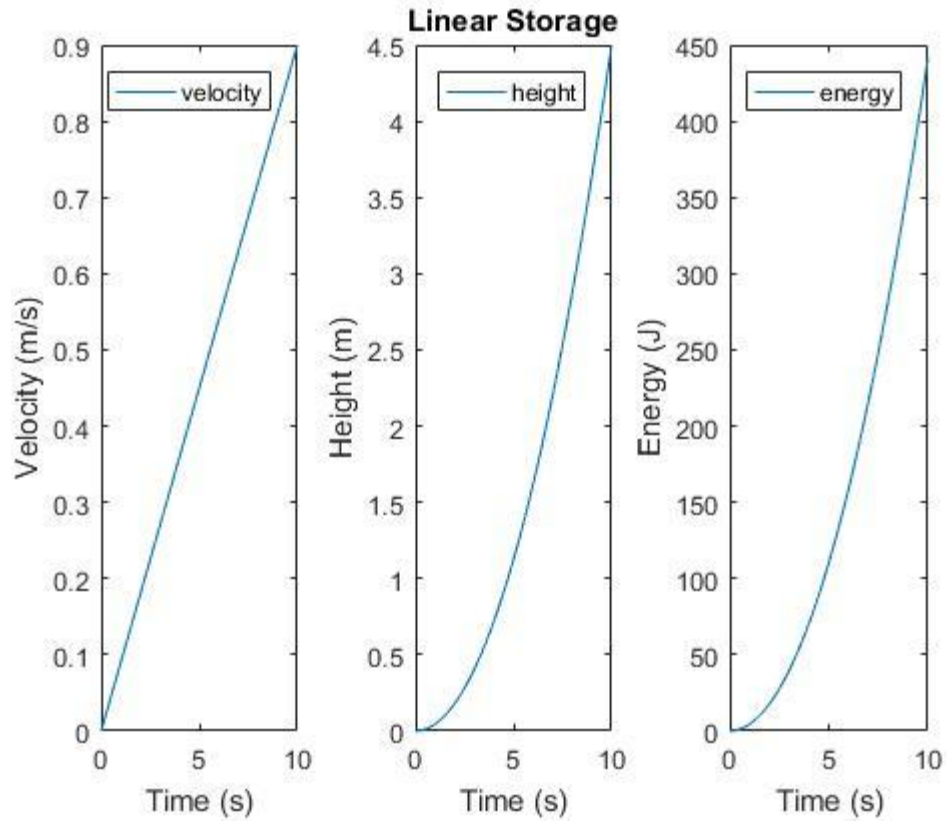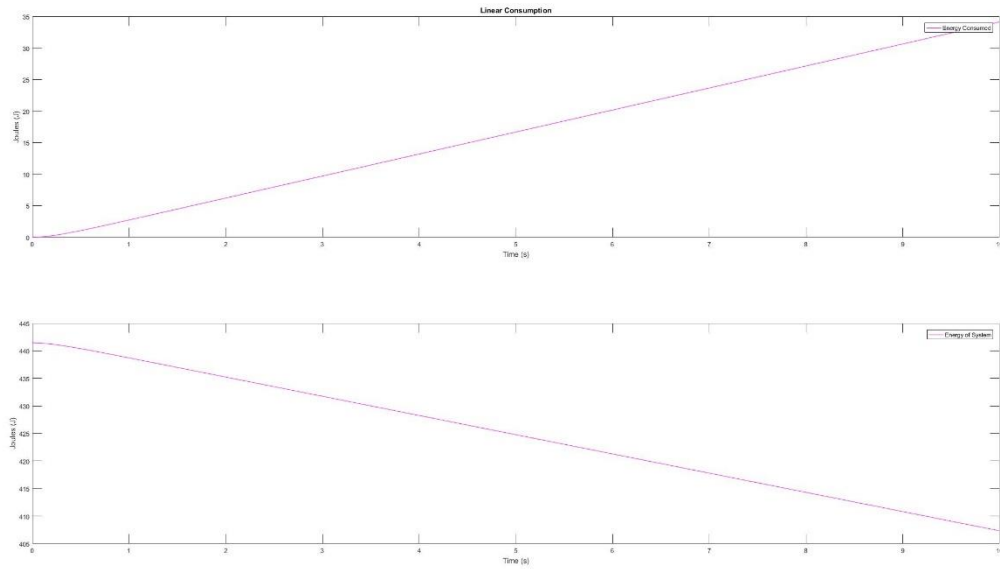
Figure 11: Plots for the Velocity, Height, Energy vs Time

Linear Consumption

The energy that was stored from above was then used to generate the output of the system. Again, using MATLAB's ode45 to generate a linear output, the following graphs were determined:

The first graph represents the amount of energy the system has been used in a given amount of time. The second graph builds on this and shows the net energy of the system over time. This second graph looks as expected as it linearly decreases with time, proportionally to height in the equation

$$potential\ energy = m \times g \times h$$

Linear model outputs

The purpose of this device to pump water through a filter, therefore the output of the system would be the outward flow rate. The flow rate determines the amount of water that can be filtered over a period of time, as this will govern how much water has been filtered. The simulation was initially tested using a combination of estimated and random numbers. But after developing the design paramters, these numbers were switched out and replaced with realistics number. This change of values changed the overall shape of a few of the graphs, and is shown below:
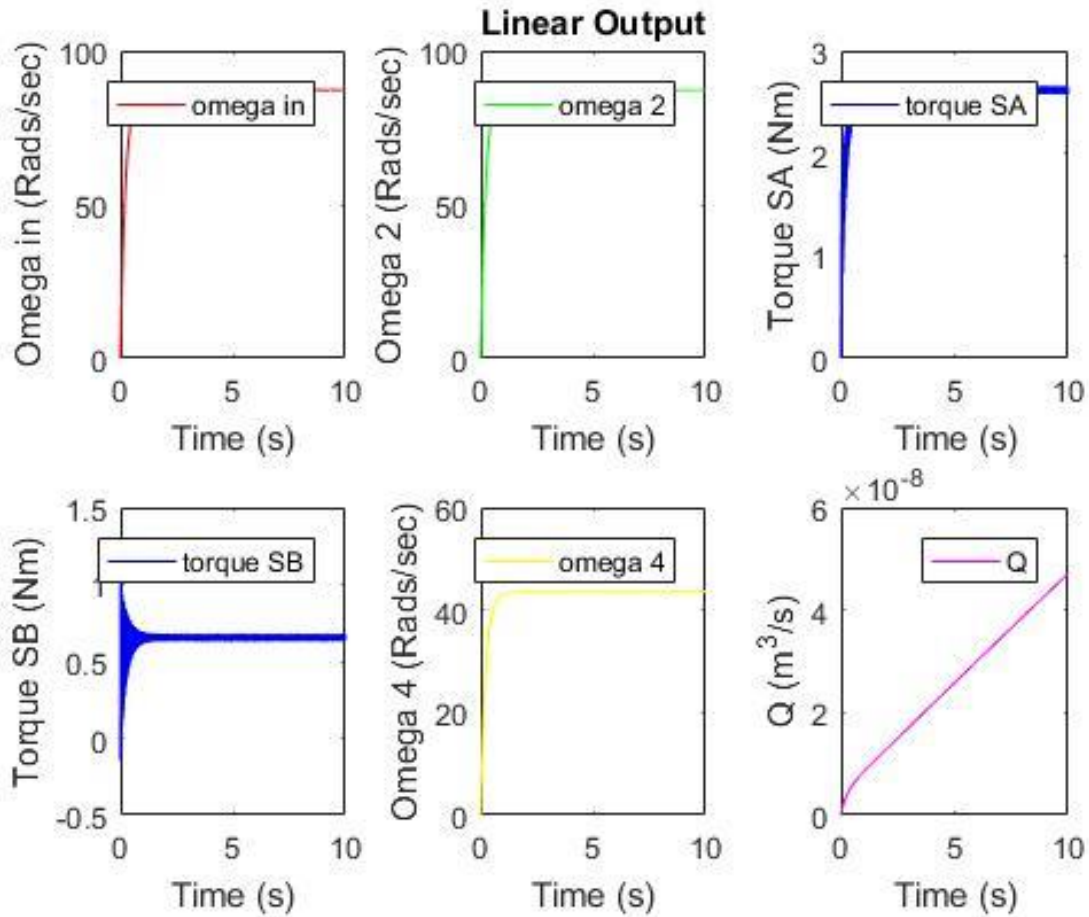
Figure 12 graphs of the linear model using the experimental data LM_EV

These above graphs represent the state variables of the system, and how each variable changes with time. As shown in figure 11, some of the outputs of the state model produce a behaviour that is to be expected. The angular velocities (omega in, 2 and 4) as well as the torque of shaft A drastically increase in value but taper off as the system approaches an equilibrium point. The torque of shaft B and the flow rate out however do not behave as anticipated, where the torque of shaft B rapidly oscillates in the beginning. While not ideal, the behaviour is not as incorrect as the output of the system. The flow rate out linearly increases after reaching a point of equilibrium. This is not supposed to happen as when the system reaches equilibrium, the flow rate should be constant.
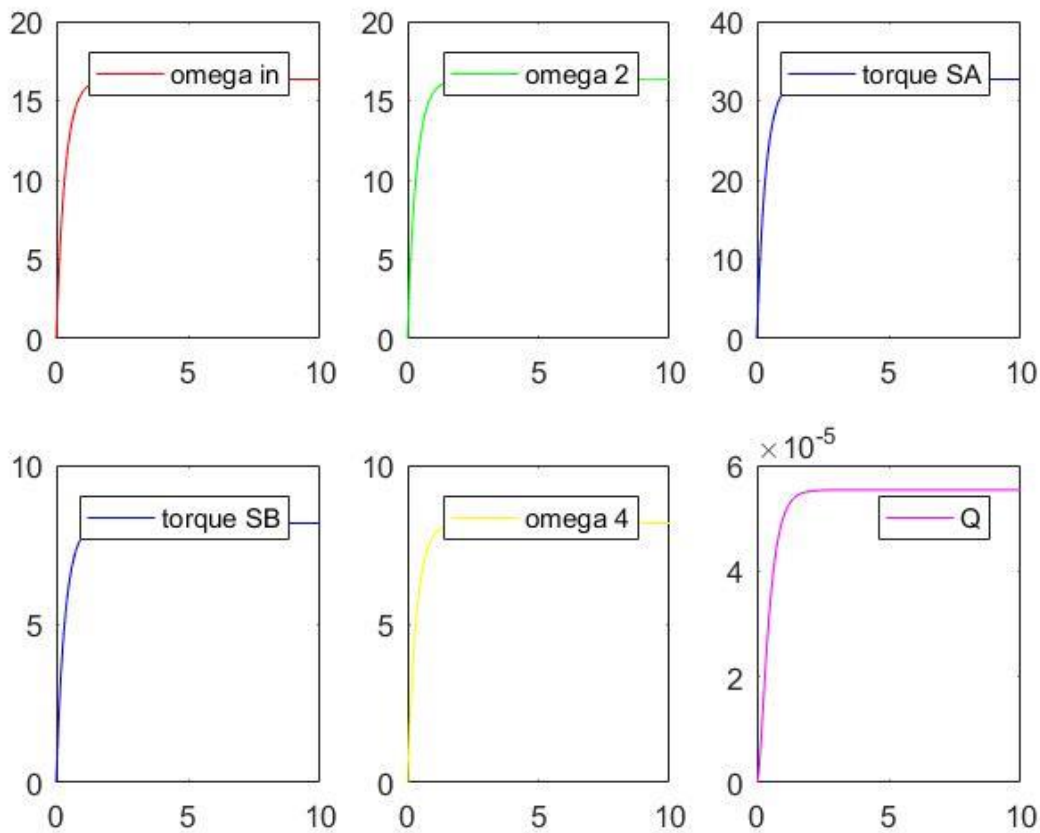
*Figure 13 graphs of the linear model using the original values LM_OGV*

When a new set of values are inputted, the simulation appears to work. The simulated model describes the behavior of the state models in a manner that would behave to the expectations. All the values initially spike up in value as all initial positions are equal to zero. However, all elements, at the same rate, decrease the rate of change, eventually plateauing at a certain time. This would be what the system should do, as the desired model assumed a linear interaction between every component where the values are almost scalar values of one another at any given time.

Linearized output

When determining which component should be given nonlinearities, it was decided that the nonlinearity of the filter was an ideal element to linearize and model. The non-linearity of the resistance of the filter directly affects the flow rate of the turbine, therefore it was wise to linearize the model about this point.

After this step, the linearization process began. This process started by finding the operating point of the system. This can be clearly seen in Appendix B. After this step, the system was

linearized about this operating point, this can additionally be seen in Appendix B. Using this approach the linearized state space system could be found, and then was implemented in MatLAB. The following graphs illustrate the linearized system:
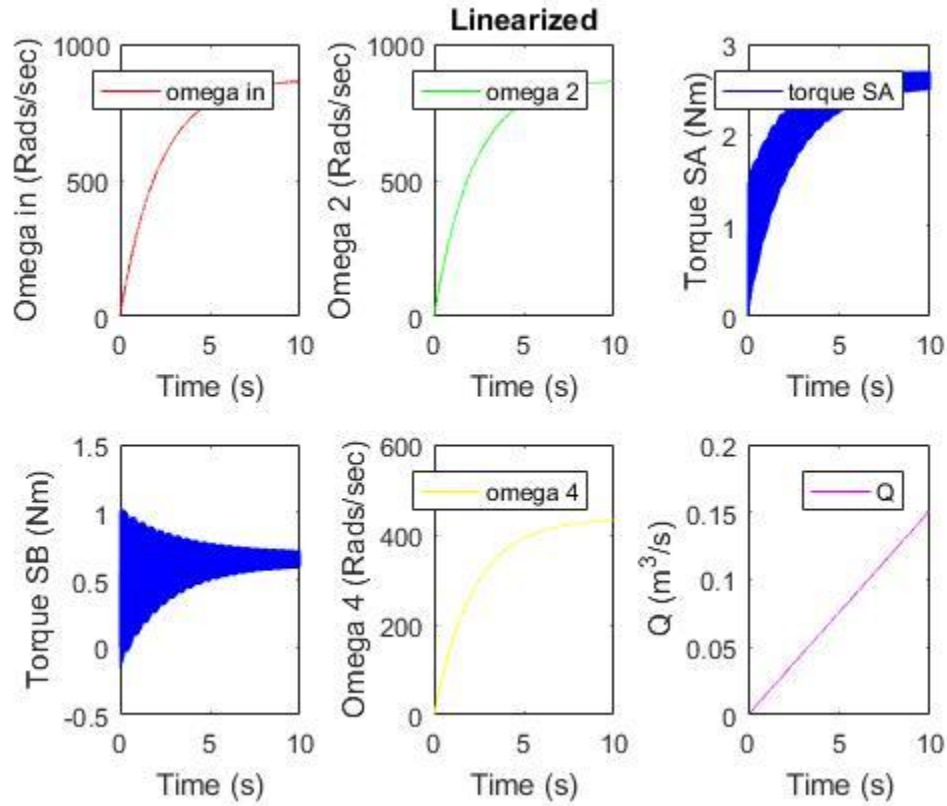
As one can see this model is similar to the previous model, however it varies slightly still. The toques are now fluctuating more than before, however the general shape of the torque graphs, in addition to the omega and flow rate graphs are similar to that of before.
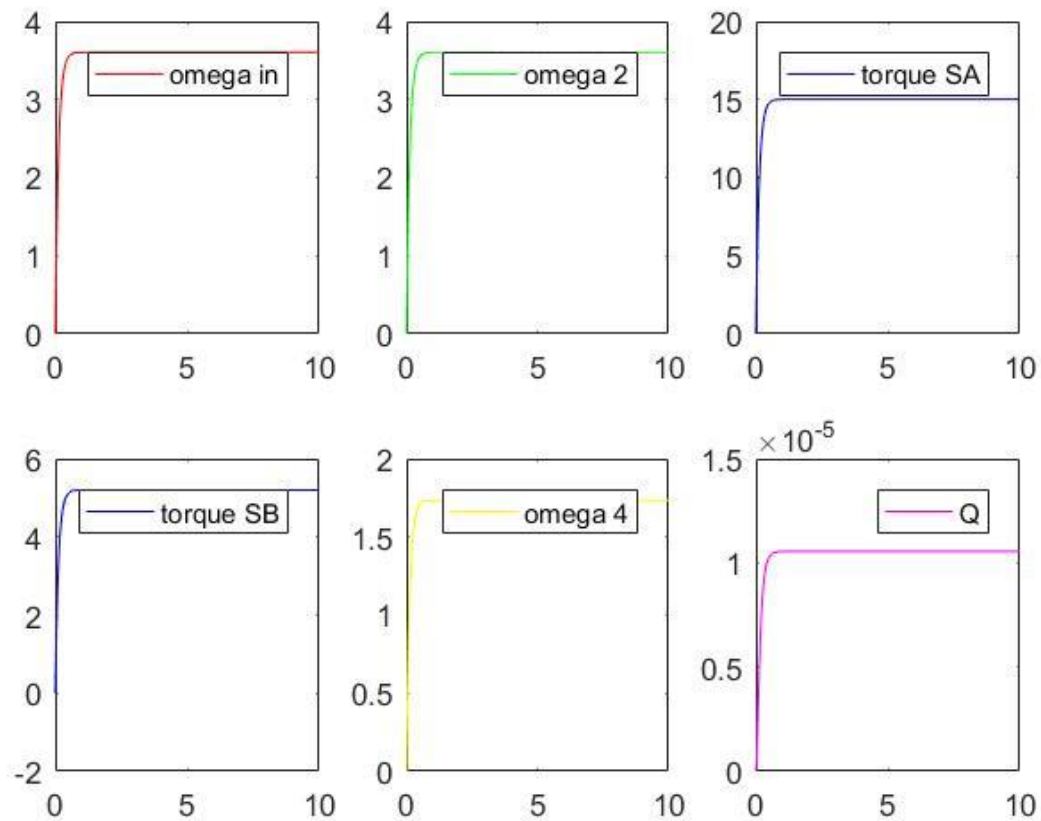
Non-linear outputs

Figure 14: graphs of the non- linear model using the original values NLM_OGV

It is more complex to analyze the non-linear models, as the effects of non-linear elements can create unique and difficult to anticipant results. With the original values, the system appears to be practically identical in shape to the linear model. However, the levels in which the outputs plateau at are different, indicating the non-linear elements influence the resulting outputs.

The model designed was not able to process the initial values presented in the design parameters. When running the MATLAB code, it would run for a full 5 minutes without producing results, much slower than the runtime of the original values.

Design Reflection/Conclusion

Although camping does provide amusement, it isn't without risk. As one goes into the great outdoors, one must be prepared to deal with the consequences that a lack of amenities can cause. Moreover, as the level of technology available for camper's increases, the dangers and consequences of straying farther and furth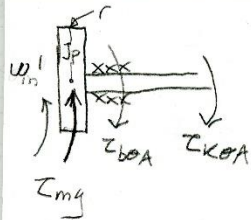er away from society become less and less. Therefore, by creating a device which could help purify water for campers, no matter the location, or the surrounding environment, one can truly be safe a sound during the camping process. As this concept developed

The experimental data used to simulate the model plotted very questionable data, not representative of what our outputs were to be expected. This could be due to the state equations used to set up, or perhaps due to the fact that the physical properties of the designs may not have been ideally designed.

References

[1]"Weather Maps - Province of British Columbia", *Www2.gov.bc.ca*, 2017. [Online]. Available: https://www2.gov.bc.ca/gov/content/safety/wildfire-status/fire-danger/fire-weather/weather-maps. [Accessed: 25- Nov- 2017].

[2]*For.gov.bc.ca*, 2017. [Online]. Available: https://www.for.gov.bc.ca/hfd/pubs/docs/lmh/Lmh66/Lmh66_ch03.pdf. [Accessed: 30- Nov- 2017].

[3]2017. [Online]. Available: https://www.currentresults.com/Weather/Canada/British-Columbia/precipitation-annual-average.php. [Accessed: 30- Nov- 2017].

[4]"Daily Data Report for October 1999 - Climate - Environment and Climate Change Canada", *Climate.weather.gc.ca*, 2017. [Online]. Available: http://climate.weather.gc.ca/climate_data/daily_data_e.html?hlyRange=%7C&dlyRange=1970-05-01%7C1999-11-30&mlyRange=1970-01-01%7C1999-11-01&StationID=1308&Prov=BC&urlExtension=_e.html&searchType=stnProv&optLimit=yearRange&StartYear=1840&EndYear=2017&selRowPerPage=25&Line=0&Month=10&Day=1&lstProvince=BC&timeframe=2&Year=1999. [Accessed: 26- Nov- 2017].

[5]"Modulus of Rigidity of some Common Materials", *The Engineering ToolBox*, 2017. [Online]. Available: https://www.engineeringtoolbox.com/modulus-rigidity-d_946.html. [Accessed: 11- Nov- 2017].

[6]"Ropes", *University of Cambrige*, 2017. [Online]. Available: http://www-materials.eng.cam.ac.uk/mpsite/short/OCR/ropes/default.html. [Accessed: 01- Dec- 2017].

[7]"Hydraulic Filtration Product Guide", *Google.ca*, 2017. [Online]. Available: https://www.google.ca/url?sa=t&rct=j&q=&esrc=s&source=web&cd=1&ved=0ahUKEwjG9vnEjuDXAhUV4GMKHUVfD3cQFghBMAA&url=https%3A%2F%2Fwww.donaldson.com%2Fcontent%2Fdam%2Fdonaldson%2Fengine-hydraulics-bulk%2Fcatalogs%2FHydraulic%2FNorth-America%2FF112100-ENG%2FHyd. [Accessed: 01- Dec- 2017].

[8]"IAPWS 2008,", *The International Association for the Properties of Water and Steam,*, 2017. [Online]. Available: http://www.iapws.org/relguide/visc.pdf. [Accessed: 01- Nov- 2017

Appendix A
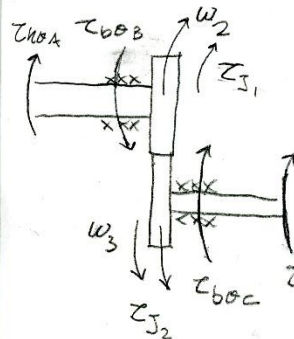

$$\tau_{J_P} = \tau_{mg} - \tau_{b\theta A} - \tau_{k\theta A}$$

$$\tau_{J_P} = w_{in}' J_P \qquad \tau_{b\theta A} = b\theta_A w_{in}$$

$$\tau_{mg} = r\, mg$$

$$w_{in}' J_P = rmg - b\theta_A w_{in} - \tau_{k\theta A}$$

$$w_{in}' = \frac{rm}{J_P} g - \frac{b\theta_A}{J_P} w_{in}' - \frac{1}{J_P} \tau_{k\theta A}$$

w_3 is in the opposite direction as w_2

$$\tau_{J_1} = w_2' J_1$$
$$\tau_{J_2} = w_3' J_2$$

Decided: $\boxed{\eta\, w_2 = w_3 \quad \& \quad \eta\, w_2' = w_3'}$

$$\eta\, w_2' = w_3' \quad \therefore \quad \tau_{J_2} = \eta\, w_2' J_2 \hookrightarrow \text{Only true if } \frac{d\theta_2}{dt} = \eta\, \alpha \quad \theta = t^2$$

$$\tau_{J_1} + \tau_{J_2} = w_2' J_1 + \eta\, w_2' J_2 \to = w_2'(J_1 + \eta J_2) \qquad \begin{array}{l}\theta' = 2t \\ \theta' = 2\end{array}$$

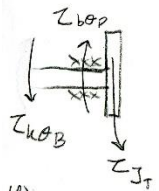$$\tau_{J_1} + \tau_{J_2} = (J_1 + \eta J_2) w_2'$$

$$\tau_{J_1} + \tau_{J_2} = \tau_{k\theta A} - \tau_{b\theta B} - \tau_{b\theta C} - \tau_{k\theta B} \qquad J_1 + J_2 + J_1\eta + J_2\eta$$

$$\tau_{b\theta B} = b\theta_B\, w_2$$

$$\tau_{b\theta C} = b\theta_C\, w_3 = b\theta_C\, \eta\, w_2$$

$$\therefore (J_1 + \eta J_2) w_2' = \tau_{k\theta A} - \tau_{k\theta B} - b\theta_B\, w_2 - b\theta_C\, \eta\, w_2$$

$$w_2' = \frac{1}{J_1 + \eta J_2} \tau_{k\theta A} - \frac{1}{J_1 + \eta J_2} \tau_{k\theta B} - \frac{b\theta_B + b\theta_C\, \eta}{J_1 + \eta J_2}\, \theta_2'$$

$$\tau_{J_T} = w_4' J_T \qquad\qquad w_4' J_T = \tau_{k\theta B} - b\theta_D\, w_4$$

$$\tau_{b\theta D} = b\theta_D\, w_4 \qquad\qquad w_4' = \frac{1}{J_T} \tau_{k\theta B} - \frac{b\theta_D}{J_T} w_4$$

$$\tau_{k\theta A}' = k\theta_A\, w_{in} - k\theta_A\, w_2$$
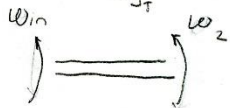
$$\tau_{k\theta B}' = k\theta_B\, \eta\, w_2 - k\theta_B\, w_4$$

Model is true if $\theta = t^2, \theta' = 2t, \theta'' = 2$
$\to$ acceleration is constant
This is true because the input is gravity, a constant.

Appendix B

$$
\begin{bmatrix} \frac{d\omega_{in}}{dt} \\ \frac{d\omega_2}{dt} \\ \frac{d\tau_{K\theta A}}{dt} \\ \frac{d\tau_{K\theta B}}{dt} \\ \frac{d\omega_4}{dt} \\ \frac{dQ}{dt} \end{bmatrix}
=
\begin{bmatrix}
-\frac{b_{\theta A}}{J_P} & 0 & -\frac{1}{J_P} & 0 & 0 & 0 \\
0 & \frac{-b_{\theta B}-b_{\theta A}G_r}{J_1+J_2G_r} & \frac{1}{J_1+J_2G_r} & \frac{-1}{J_1+J_bG_r} & 0 & 0 \\
K_{\theta A} & -K_{\theta A} & 0 & 0 & 0 & 0 \\
0 & K_{\theta B}G_r & 0 & 0 & -K_{\theta B} & 0 \\
0 & 0 & 0 & \frac{1}{J_t} & -\frac{b_{\theta D}}{J_t} & 0 \\
0 & 0 & 0 & \frac{K_1}{I_{eq}} & -\frac{b_{\theta D}}{I_{eq}} & E
\end{bmatrix}
+
\begin{bmatrix} \frac{r_p m}{J_P} \\ 0 \\ 0 \\ 0 \\ 0 \\ 0 \end{bmatrix} g
$$

$$E = -\frac{1\times10^9 Q + 1\times10^7 + Z}{I_{eq}} \qquad Z = R_h + R_v$$

---

1) Find $\bar{q}$ by setting $\dot{q}=0$

$$\frac{d\omega_{in}}{dt} = 0 = -b_{\theta A}\overline{\omega_{in}} - \overline{\tau_{K\theta A}} + r_p mg \;\Rightarrow\; \overline{\omega_{in}} = \frac{-\overline{\tau_{K\theta A}} + r_p mg}{b_{\theta A}} \quad \text{①}$$

$$\frac{d\omega_2}{dt} = 0 = (-b_{\theta B}-b_{\theta G}G_r)\overline{\omega_2} + \overline{\tau_{K\theta A}} - \overline{\tau_{K\theta B}} \;\Rightarrow\; \overline{\omega_2} = \frac{-\overline{\tau_{K\theta A}} + \overline{\omega_4}\,b_{\theta B} = \overline{\omega_2}}{-b_{\theta B} - b_{\theta G}G_r} \quad \text{②}$$

$$\frac{d\tau_{K\theta A}}{dt} = 0 = K_{\theta A}\overline{\omega_{in}} - K_{\theta A}\overline{\omega_2} \;\Rightarrow\; \overline{\omega_{in}} = \overline{\omega_2} \quad \text{③}$$

$$\frac{d\tau_{K\theta B}}{dt} = 0 = K_{\theta B}G_r\overline{\omega_2} - K_{\theta B}\overline{\omega_4} \;\Rightarrow\; \overline{\omega_4} = G_r\overline{\omega_2} \quad \text{④}$$

$$\frac{d\omega_4}{dt} = 0 = \overline{\tau_{K\theta B}} - b_{\theta D}\overline{\omega_4} \;\Rightarrow\; \overline{\tau_{K\theta B}} = \overline{\omega_4}\,b_{\theta B} \quad \text{⑤}$$

$$\frac{dQ}{dt} = 0 = K_1\overline{\tau_{K\theta B}} - b_{\theta D}\overline{\omega_4} + 1\times10^9\bar{Q}^2 - 1\times10^7\bar{Q} - Z \;\Rightarrow\; \bar{Q} = -5\times10^{-3} + \sqrt{\frac{1\times10^{14} - 4\times10^9(-Z + K_1\overline{\tau_{K\theta B}} - b_{\theta D}\overline{\omega_4})}{-2\times10^9}} \quad \text{⑥}$$

sub ⑤ & ① into ②

$$\frac{\overline{\omega_2}\, b\theta_A - r_p\, mg + G_r\, \overline{\omega_2}\, b\theta_B}{-b\theta_B - b\theta_C\, G_r} = \overline{\omega_2} \Rightarrow \quad ⑦ \quad \overline{\omega_2} = \frac{r_p\, mg}{2b\theta_B + b\theta_C G_r + G_r\, b\theta_B}$$

$$\overline{\omega_2} = \frac{r_p\, mg}{2b\theta_B + G_r(b\theta_C + b\theta_B)}$$

sub ④ into ⑤

$$\overline{v_{k\theta B}} = G_r\, b\theta_B\, \overline{\omega_2} \quad ⑧$$

sub ④ & ⑧ into ⑥

$$-5\times10^{-3} + \sqrt{\frac{1\times10^{14} - 4\times10^{9}\left(-Z + K_1\left(G_r\, b\theta_B\, \overline{\omega_2}\right) - b\theta_D\left(G_r\, \overline{\omega_2}\right)\right)}{-2\times10^{9}}} \quad ⑨$$

sub ⑦ into ⑨

$$-5\times10^{-3} + \sqrt{\frac{1\times10^{14} - 4\times10^{9}\left(-Z + \frac{(K_1\, b\theta_B - b\theta_D)\, G_R\, r_p\, mg}{2b\theta_B + G_r(b\theta_C + b\theta_B)}\right)}{-2\times10^{9}}} = \overline{Q}$$

$$\overline{Q} \Rightarrow \quad 10^7 + \sqrt{\frac{10^{14} - 4\times10^{9}\left(-Z + \frac{(K_1\, b\theta_B - b\theta_D)\, G_R\, r_p\, mg}{2b\theta_B + G_r(b\theta_C + b\theta_B)}\right)}{-2\times10^{9}}}$$

36

$$\dot{\hat{q}} = \frac{\partial f(\bar{q}, \bar{r}, \bar{t})}{\partial \bar{q}} \hat{q} + \frac{\partial f(\bar{q}, \bar{r}, \bar{t})}{\partial \bar{r}} \hat{r}$$

$$\hat{q} = [\widehat{w_{in}} \quad \widehat{w_2} \quad \widehat{\tau_{k\theta A}} \quad \widehat{\tau_{k\theta B}} \quad \widehat{w_A} \quad \hat{Q}] \qquad \hat{r} = \hat{g}$$

$$\dot{\hat{Q}} = 0 \widehat{w_{in}} + 0 \widehat{w_2} + 0 \widehat{\tau_{k\theta A}} + \frac{K_1}{I_{eq}} \widehat{\tau_{k\theta B}} - \frac{b_{OD}}{I_{eq}} \widehat{w_A} + \left(\frac{-2 \times 10^9 \bar{Q} + 1 \times 10^7 + z}{I_{eq}} \right) \hat{Q}$$

All other state equations stay the same
i.e. $\widehat{w_{in}} = w_{in}$

$$\dot{w}_{in}(t) = \overline{w_{in}} + \widehat{w_{in}}(t)$$
$$w_2(t) = \overline{w_2} + \widehat{w_2}(t)$$
$$\tau_{k\theta A}(t) = \overline{\tau_{k\theta A}} + \widehat{\tau_{k\theta A}}(t)$$
$$\tau_{k\theta B}(t) = \overline{\tau_{k\theta B}} + \widehat{\tau_{k\theta B}}(t)$$
$$w_A(t) = \overline{w_A} + \widehat{w_A}(t)$$
$$Q(t) = \overline{Q} + \hat{Q}(t)$$